

A high-power dual-crystal Tm: YLF laser with 80.9% slope efficiency

Yinfei Liu(刘寅飞), Jiajun Song(宋贾俊), Yujie Peng(彭宇杰), Guanguang Gao(高贯光), Liya Shen(沈丽雅), Junze Zhu(朱君泽), Tianze Xu(徐天泽), and Yuxin Leng(冷雨欣)
Citation: Chin. Phys. B, 2026, 35 (**3**): 034202. DOI: 10.1088/1674-1056/adf4ac
http://cpb.iphy.ac.cn; http://iopscience.iop.org/cpb

What follows is a list of articles you may be interested in

High efficiency and high transmission asymmetric polarization converter with chiral metasurface in visible and near-infrared region

Yuhang Gao(高雨航), Yu Tian(田宇), Qingguo Du(杜庆国), Yuanli Wang(王原丽), Qin Fu(付琴), Qiang Bian(卞强), Zhengying Li(李政颖), Shuai Feng(冯帅), and Fangfang Ren(任芳芳)
Chin. Phys. B, 2023, 32 (**7**): 074201. DOI: 10.1088/1674-1056/acb9eb

High efficiency of Brillouin scattering behavior in single-mode Ge-As-Se-Te fibers at 2 μm

Yue Fu(付悦), Shi-Xun Dai(戴世勋), Lu-Lu Xu(徐路路), Yao-Jun Fang(方耀俊), Ying-Ying Wang(王莹莹), Kai Jiao(焦凯), and Xun-Si Wang(王训四)
Chin. Phys. B, 2023, 32 (**5**): 054206. DOI: 10.1088/1674-1056/ac9a3a

High efficiency of broadband transmissive metasurface terahertz polarization converter

Qiangguo Zhou(周强国), Yang Li(李洋), Yongzhen Li(李永振), Niangjuan Yao(姚娘娟), and Zhiming Huang(黄志明)
Chin. Phys. B, 2023, 32 (**2**): 024201. DOI: 10.1088/1674-1056/ac6db7

Large aperture phase-coded diffractive lens for achromatic and 16° field-of-view imaging with high efficiency

Gu Ma(马顾), Peng-Lei Zheng(郑鹏磊), Zheng-Wen Hu(胡正文), Suo-Dong Ma(马锁冬), Feng Xu(许峰), Dong-Lin Pu(浦东林), and Qin-Hua Wang(王钦华)
Chin. Phys. B, 2022, 31 (**7**): 074210. DOI: 10.1088/1674-1056/ac560c

A narrow-linewidth continuous wave Ho：$YALO_3$ laser with Fabry–Perot etalons

Yang Xiao-Tao (杨晓涛)
Chin. Phys. B, 2014, 23 (**3**): 034207. DOI: 10.1088/1674-1056/23/3/034207

A high-power dual-crystal Tm:YLF laser with 80.9% slope efficiency

Yinfei Liu(刘寅飞)[1,2], Jiajun Song(宋贾俊)[1,†], Yujie Peng(彭宇杰)[1,3,‡], Guanguang Gao(高贯光)[1], Liya Shen(沈丽雅)[1,4], Junze Zhu(朱君泽)[1,2], Tianze Xu(徐天泽)[1,2], and Yuxin Leng(冷雨欣)[1,3,§]

[1] *State Key Laboratory of Ultra-intense laser Science and Technology, Shanghai Institute of Optics and Fine Mechanics (SIOM), Chinese Academy of Sciences (CAS), Shanghai* 201800, *China*

[2] *Center of Materials Science and Optoelectronics Engineering, University of Chinese Academy of Sciences, Beijing* 100049, *China*

[3] *School of Physics and Optoelectronic Engineering, Hangzhou Institute for Advanced Study, University of Chinese Academy of Sciences, Hangzhou* 310024, *China*

[4] *School of Physical Science and Technology, ShanghaiTech University, Shanghai* 201210, *China*

(Received 21 April 2025; revised manuscript received 10 June 2025; accepted manuscript online 28 July 2025)

We demonstrate a high-power continuous-wave Tm:YLF laser with exceptional efficiency, achieved through laser diode end-pumping of dual Tm:YLF crystals in a thermally insensitive resonator at room temperature. The performance of the Tm:YLF laser system has been thoroughly investigated, covering output power, efficiency, power stability, and beam quality. A maximum output power of 45.85 W was achieved with an absorbed pump power of 60.89 W. The slope efficiency and absorbed-to-optical conversion efficiency were 80.9% and 75.3%, respectively. The laser exhibits excellent stability, with an RMS power stability of 0.33%. The beam quality (M^2) of the Tm:YLF laser in the horizontal and vertical directions were 1.01 and 1.05, respectively. This high-performance laser source is ideal for pumping holmium-doped crystals to generate 2-μm laser and mid-infrared laser generation via nonlinear optical processes.

Keywords: Tm:YLF, 2-μm laser, high efficiency

PACS: 42.55.Xi, 42.60.–v, 42.55.–f, 42.55.Ah

DOI: 10.1088/1674-1056/adf4ac **CSTR:** 32038.14.CPB.adf4ac

1. Introduction

Lasers in the 2-μm wavelength range have enabled transformative applications across multiple disciplines, including atmospheric sensing, precision materials processing, and minimally invasive medical procedures.[1–5] The 2-μm laser's eye-safe operation and strong water absorption make it ideal for medical applications, enabling precise tissue ablation with enhanced hemostasis and minimized collateral damage.[6,7] Furthermore, the 2-μm laser is an excellent pump source for mid-infrared (MIR) generation via nonlinear frequency conversion, including optical parametric oscillation (OPO) and optical parametric amplification (OPA).[1,8,9] Compared to conventional 1-μm pump sources, 2-μm driven nonlinear processes enable broader phase-matching bandwidths, facilitating tunable mid-infrared generation across wider spectral ranges. Furthermore, the laser-induced damage threshold of optical materials exhibits a positive wavelength dependence, significantly enhancing the feasibility of high-power 2-μm laser development and their practical deployment in demanding applications.[10]

Several methods exist for generating 2-μm lasers, including optical parametric oscillation, optical parametric amplification, and other nonlinear optical processes, though these often suffer from inefficiency and low maximum output power.[11] Direct 2-μm laser generation has been successfully demonstrated using thulium (Tm^{3+})-doped, holmium (Ho^{3+})-doped, and Tm/Ho co-doped gain media, offering a viable alternative to nonlinear conversion approaches.[12,13] Notably, pumping Ho-doped gain media with 1.9-μm Tm-lasers to generate 2-μm light offers exceptionally high quantum efficiency, as the pump wavelength closely matches the emission wavelength.[14] Furthermore, Tm and Ho-doped gain media provide higher efficiency, greater output power, and more stability compared to nonlinear optical methods. Consequently, advancing Tm^{3+} laser technology represents a critical pathway for developing high-performance 2-μm laser systems, combining the benefits of direct generation with superior power scaling potential.

Research on rare earth ions as gain media has rapidly advanced in recent years, with Tm ions emerging as a key candidate for next-generation ultra-intense laser systems in the 2-μm wavelength range. This is due to Tm's long upper energy level lifetime, broad emission spectrum, weak thermal lensing, and lower thermo-optic coefficient.[15–20] Tm-based systems, including Tm:YLF, are typically pumped by commercial laser diodes (LD) with a central wavelength around 800 nm. When a Tm ion in the ground state absorbs a pump photon, it is excited to the $^3H_4$ energy level via the $^3H_6 \rightarrow {}^3H_4$ transi-

†Corresponding author. E-mail: songjiajun@siom.ac.cn

‡Corresponding author. E-mail: yjpeng@siom.ac.cn

§Corresponding author. E-mail: lengyuxin@siom.ac.cn

© 2026 Chinese Physical Society and IOP Publishing Ltd. All rights, including for text and data mining, AI training, and similar technologies, are reserved.

tion. The ion then decays from the $^3H_4$ to the $^3F_4$ energy level through a photonic self-quenching process, simultaneously releasing a photon that can excite another nearby Tm ion from the ground state to the upper energy level.[10] This process, known as cross-relaxation, occurs in highly doped samples. Notably, the theoretical quantum efficiency of Tm-based systems is twice that of conventional gain media like Ti:sapphire and Yb:YAG, due to the one-for-two process. Ultimately, the Tm ion in the $^3F_4$ energy level relaxes to the ground state, emitting laser light with a central wavelength around 1.9 μm.

The Tm:YLF crystal also possesses several advantageous properties, such as natural birefringence, a low and negative thermo-optic coefficient, a small refractive index, and a long upper-state lifetime. These properties make Tm:YLF an excellent gain medium for high-power, high-energy laser systems.[9,16] However, the relatively low thermal conductivity of Tm:YLF crystals poses a critical challenge for heat dissipation in high-power operation. This thermal limitation necessitates maintaining relatively low Tm-ion doping concentrations. Furthermore, low doping concentrations reduce pump absorption efficiency, leading to significant pump power losses. In recent decades, significant research efforts have been devoted to developing 1.9-μm Tm:YLF lasers, as evidenced by numerous experimental studies.[21–25] In 2000, Budni *et al*. achieved a 22-W continuous-wave Tm:YLF laser output pumped by 60-W diode-laser, with an optical to optical conversion efficiency of 37%.[26] In 2008, Duan *et al*. demonstrated a 9.8-W Tm:YLF laser output with an input pump power of 24 W, corresponding to optical conversion efficiency of 40.9% and slope efficiency of 51.4%.[6] And in 2015, Ding *et al*. reported a diode-end-pumped dual crystal Tm:YLF laser with an output power of 50.3 W, corresponding to the optical-to-optical efficiency of 32.1% and slope efficiency of 41.6%.[8] The same year, Shen *et al*. demonstrated a continuous-wave Tm:YLF laser using two slab crystals pumped by four fiber-coupled laser diodes, achieving a maximum output power of 108 W, corresponding to a slope efficiency of 39.0% and an optical-to-optical conversion efficiency of 35.5 % with respect to the incident pump power.[27] Recently, Wei *et al*. demonstrated a 202-W Tm:YLF slab laser using a reflecting volume Bragg grating as the output coupler, the corresponding slope efficiency and optical-to-optical conversion efficiency were 39.7% and 36.5%, respectively.[28] While this advancement pushes the maximum output power of Tm:YLF slab lasers beyond the 100-W threshold, challenges remain, such as high costs (due to multiple pump sources), complex structures, and relatively low efficiency. Additionally, Tm:YLF crystals are sensitive to cooling temperatures and are somewhat influenced by the pump source,[29–31] prompting research into cryogenic cooling for Tm:YLF lasers and the use of Ti:sapphire lasers as pump sources.[10] For instance, Adrian Alles *et al*. demonstrated a cryogenic Tm:YLF laser in 2023, achieving a maximum output power of 6.5 W at 80 K, corresponding to a slope efficiency of 66.0% with respect to the absorbed power.[7] Moreover, in 2022, Umit Demirbas *et al*. conducted a detailed study on the continuous-wave lasing performance of Tm:YLF crystals with doping concentrations ranging from 2% to 6%, pumped by diode and Ti:sapphire lasers at 792 nm and 780 nm, respectively. The study achieved a peak slope efficiency of about 70% with respect to absorbed pump power when using a Ti:sapphire laser to pump a 6% Tm-doped YLF crystal.[15] This is the highest efficiency of the Tm:YLF laser to date. Nevertheless, Ti:sapphire lasers are expensive and provide lower power output. To improve both optical-to-optical conversion efficiency and output power, we propose a high-efficiency Tm:YLF bulk crystal laser, which maintains a simple structure and low cost.[32,33]

This work demonstrates a high-power, continuous-wave Tm:YLF laser operating at room temperature with exceptional efficiency. Our innovative design combines dual Tm:YLF crystals in a thermally compensated cavity, single 105-μm core diameter fiber-coupled diode pumping and optimized power extraction, achieving high power and high efficiency output while maintaining excellent stability (0.33% RMS). This architecture provides significant advantages in system simplicity, cost-effectiveness, and operational robustness compared to conventional approaches. The polarization-independent absorption characteristics of Tm:YLF enable simultaneous pumping of dual crystals using a single laser diode (LD), thereby significantly improving pump source utilization efficiency. A thermally stable cavity design was employed to offset Tm:YLF's thermal lensing effects on power output and beam quality. To optimize laser output power, we implemented an efficient output coupling control scheme using a quarter-wave plate (QWP) and thin-film polarizer (TFP) combination. Under an incident pump power of 130 W and an absorbed pump power of approximately 61 W, the maximum continuous-wave output power of 45.85 W at 1880 nm was achieved, corresponding to a slope efficiency and absorbed-to-optical conversion efficiency were 80.9% and 75.3%, respectively. The beam quality (M^2) factors were 1.01 and 1.05 in horizontal and vertical directions, respectively.

2. Experimental setup

The layout of the proof-of-principle experimental setup is shown in Fig. 1(a). A commercial multi-mode fiber-coupled LD is used as the pump source, with a central wavelength and spectral bandwidth (full width at half maximum, FWHM) of 793 nm and 2.6 nm, respectively. The laser diode features a 105-μm core diameter and 0.22 numerical aperture, yielding an M^2 value of 45.8. The laser diode achieves a maximum

output power of 130 W. A spherical lens (L1) with a focal length of 20 mm is employed to collimate the pump beam. A dichroic mirror (DM1), which is high-reflection (HR) coated at 1880 nm and anti-reflection (AR) coated at 793 nm, is used to protect the LD from devastation by the back laser. The polarizing beam splitter (PBS) splits the unpolarized pump beam into two orthogonally polarized beams with equal power. A half-wave plate (HWP) rotates the p-polarized beam to s-polarization. Both resulting pump beams are then focused onto the crystals using 100-mm focal length spherical lenses (L2 and L3). The total depletion of both two polarized beams is about 3% and the input powers incident on both crystals are almost equal. The pump spot diameters within both crystals were measured to be approximately 500 μm, with corresponding Rayleigh ranges of ∼ 11 mm, as determined from characterization of the focused spots produced by lenses L2 and L3.

Both crystals are *a*-cut and optimized for lasing in $E \parallel c$ configuration of Tm:YLF, with a doping concentration of 3%. Both crystal end faces feature anti-reflection (AR) coatings optimized for 793 nm and 1880 nm. The crystal orientation is illustrated in the inset of Fig. 1(a). The crystals are thermally mounted between two water-cooled copper heat sinks using 0.05-mm indium foils, with the coolant maintained at 18 °C. The output power and efficiency increased as temperature decreased. However, we cannot lower the temperature indefinitely, as the frost will form on the surface of the crystals at low cooling water temperatures. Therefore, we set the water chiller temperature at 18 °C as a consideration of safety and stability. The crystal length is 10 mm, which aligns well with the Rayleigh length of the pump source. To improve thermal management, the crystal end faces are designed with a compact 2 mm×2 mm cross-section. All 2 mm×10 mm planar surfaces of both crystals and copper heat sinks are polished and gold-coated (Au) to optimize thermal contact uniformity and efficiency. However, Tm:YLF exhibits a relatively low pump saturation intensity (∼ 3.27 kW/cm^2) compared to gain media like Yb:YAG, a consequence of its long upper-state lifetime. Additionally, the crystal's absorption rate decreases with increasing pump power. On the one hand, this effect primarily stems from Tm:YLF's low pump saturation intensity, which fundamentally limits achievable absorption of the pump radiation. On the other hand, the pump wavelength shift with increasing power may contribute, as the absorption cross-section varies significantly across the pump spectrum.

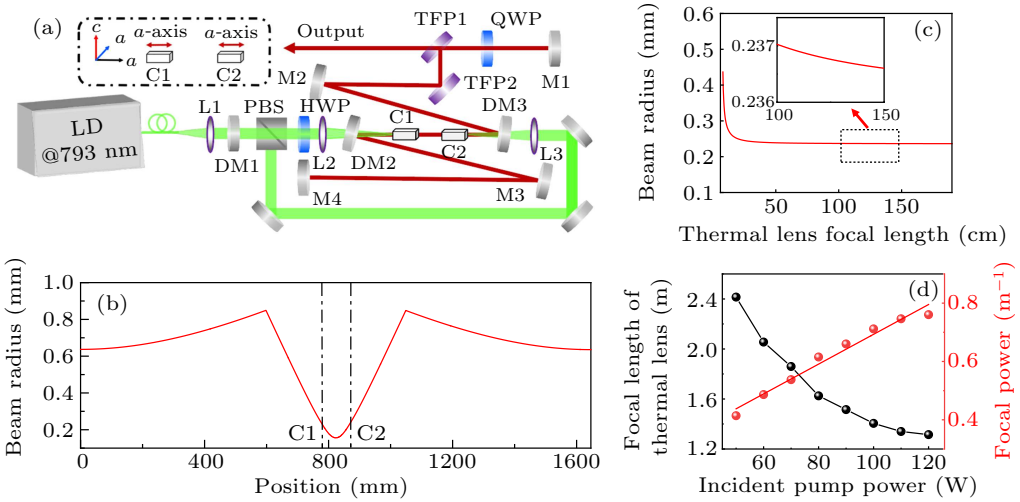


Fig. 1. (a) Layout of the experimental setup. TFP1–TFP2: thin-film polarizer; QWP: quarter wave plate; HWP: half wave plate; L1–L3: lenses; PBS: polarizing beam splitter cube; LD: laser diode; M1 and M4: plane mirrors; M2 and M3: concave mirrors with a radius of curvature of 400 mm; DM1 to DM3: dichroic mirrors; C1–C2: Tm:YLF crystals. Insets, orientation of Tm:YLF crystals used in this experiment. (b) Cavity mode distribution of the dual-crystal Tm:YLF resonant cavity. (c) Beam radius variation with different focal lengths of thermal lens. (d) Focal length of thermal lens with different incident pump powers.

An analog Z-type resonator is used for laser experiments, as shown in Fig. 1(a). The laser cavity consisted of two plane mirrors (M1, M4), two thin-film polarizers (TFPs), two concave mirrors (M2, M3), and two dichroic mirrors (DM2, DM3), both of which are identical to DM1. The total length of the resonator cavity is 1640 mm, resulting in a spot diameter of ∼ 400 μm at the central of the crystal, slightly smaller than the pump beam size. A home-made output coupler, comprising a quarter-wave plate (QWP) and a thin-film polarizer (TFP), adjusts the resonator cavity's output coupling rate. The coupling output rate is adjusted by rotating the QWP, with each angle corresponding to a distinct rate, as calibrated using a commercial laser. The cavity mode distribution is presented in Fig. 1(b). Figure 1(c) illustrates the variation of the cavity mode in the crystal as a function of the thermal lens. It is evident that the cavity mode remains nearly unchanged when the focal length of thermal lens exceeds 500 mm. Especially, the beam radius only changes from 237.0 μm to 236.6 μm when the thermal lens focal length increased from 1000 mm to 1500 mm, as shown in the inset of Fig. 1(c). Therefore, this

resonant cavity can handle higher pump power while avoiding mode mismatch for better output beam quality. To measure the thermal lens focal length in the Tm:YLF laser, we constructed a plano-plano resonator and determined the thermal lens by imaging the output coupler's beam spot size using a $4f$ optical system. The experimentally measured focal length of thermal lens in the Tm:YLF crystal at different incident pump power were depicted in Fig. 2(d). The focal length of thermal lens (black line) of Tm:YLF crystal remain over 1000 mm, even at the highest incident pump power, which further illustrated the thermal stability of the resonator cavity.

3. Results and discussion

To begin with, the pump absorption properties of the Tm:YLF crystals in our experiments were characterized due to the relatively low doping concentration, as shown in Fig. 2(a). The blue line depicted that the absorption rate dropped from 0.59 to 0.4 as the incident pump power increased from 10 W to 130 W, which suggest that the absorption rate of the 3% doping Tm:YLF is relatively low and decrease gradually with the increasing of the incident pump power due to pump saturation. The red line indicates the absorption properties under laser operating conditions. Owing to stimulated emission, the intracavity laser light balances the pump saturation, the absorption rate is a little higher than the no laser condition at the same incident pump power, which dropped from 0.59 to 0.47 as the incident pump power increases, but it remains at a relatively low level.

We then conducted Tm:YLF lasing experiments using LD pumping with a 10-mm long, 3% Tm-doped YLF crystal. Figure 2(b) depicts the measured CW lasing performance of the diode pumped Tm:YLF laser as a function of absorbed pump power, under different output coupling values ranging from 5% to 40%. The output power was characterized by a commercial power meter (Gentec-UP55N-100H-H9-D0), which were set at 793 nm and 1880 nm, respectively, when measuring the pump power and output power. The maximum output power of 45.85 W was obtained under an absorbed pump power of 60.89 W with a 13% output coupler, corresponding to a slope efficiency of 80.9% and an absorbed-to-optical conversion efficiency of 75.3%, which approaching the quantum efficiency of Tm^{3+} ions. Furthermore, there is no result shows that the slope efficiency would decrease at higher pump power, which means the output power could be further increased by raising pump power. Besides, as shown in Fig. 2(b), the 5% transmitting output coupler has higher output power at low absorbed pump power, but has poor performance at high absorbed pump power. The performance of different output coupler work at different absorbed pump power condition might not only depend on the ratio between the intracavity laser light and the output laser, but also the absolute value of the intracavity laser light. This helps explain why the low-transmitting output coupler performs better at lower incident pump power.

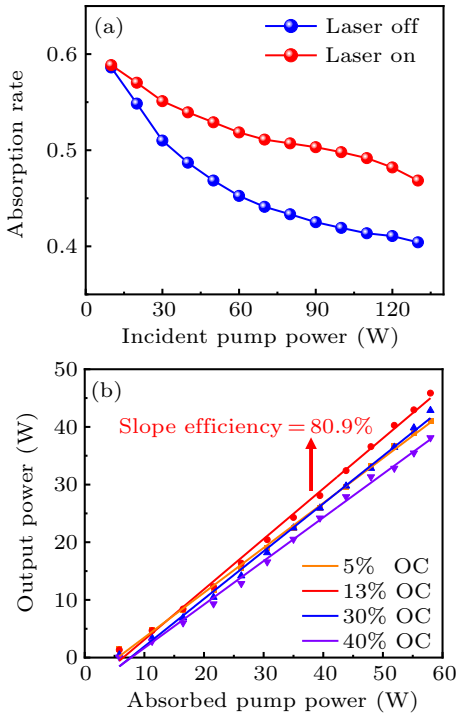


Fig. 2. (a) The absorption rate of Tm:YLF crystal, laser off (blue line) and laser on (red line). (b) Measured CW efficiency curved for the LD pumped Tm:YLF laser under different output coupling rates.

We also investigated the wavelength variations of the Tm:YLF laser by measuring its CW laser performance with different output couplers. An NIR-25s spectrum analyzer with a resolution of 3 nm was used to measure the spectrum of the output laser. The Tm:YLF crystal has two main emission peaks, which are at 1880 nm in the π direction and 1908 nm in the σ direction if no wavelength control is adopted, respectively.[34] Furthermore, the absorption cross-section and the emission cross-section in the π direction are larger than in the σ direction, which could enhance the efficiency of the Tm:YLF laser to some degree. As shown in Fig. 3, the free running laser wavelength for each output coupler is depicted. The output laser peak shifts from 1886.4 nm to 1880.0 nm with the increasing of output coupling ratio, which is universal for quasi-three-level lasers due to the higher inversion levels required to reach threshold.[15] With the increasing of the output coupler's transmission, a higher upper-state population is required to overcome the increased transmission loss. Additionally, the effective emission cross section is higher at shorter wavelength, meaning that shorter wavelength gain will hold a dominant position once population inversion is reached. Consequently, the laser output peak shifts toward shorter wavelengths as the output coupling ratio increases. The center wavelength is located at 1883.1 nm and the full width at half-maximum (FWHM) is measured to be approximately 9.2 nm at the maximum output power, which corresponding to an output coupling ratio of 13%.

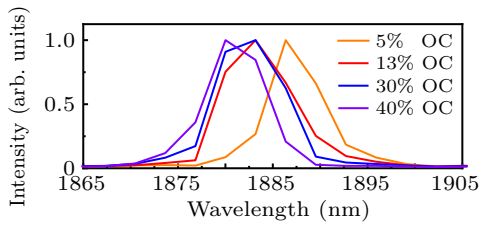


Fig. 3. Spectrum of the Tm:YLF laser at different output coupling rates.

The power stability of the output power of the Tm:YLF laser is characterized by a commercial power meter (Gentec-UP55N-100H-H9-D0). During this experiment, we observed that whether the laser system was isolated by a home-made box had a notable impact on the stability of its output power. The results showed that with the box isolation, the output power of the laser become more stable, likely due to the cover's effectiveness in reducing air fluctuations and external vibrations that could interfere with the laser's performance. When the laser system is not isolated by a cover, the RMS value is just 1.23%. As a comparison, the stability is improved to 0.33% when the system is isolated by a cover. The results are shown in Figs. 4(a) and 4(b).

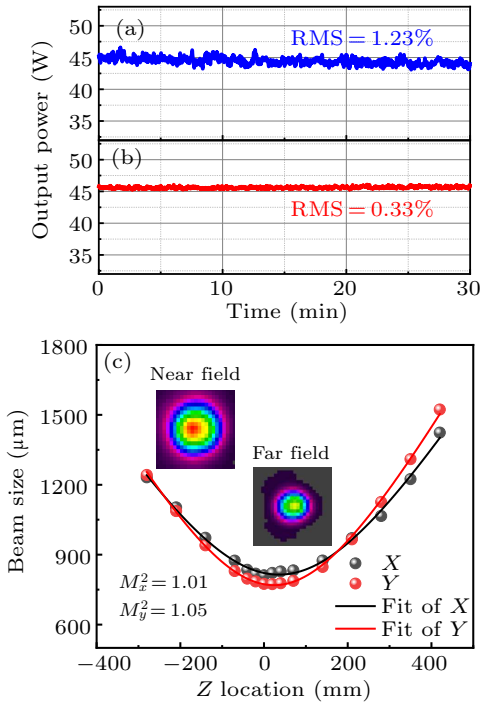


Fig. 4. (a) Power stability of the Tm:YLF laser when the laser system is not isolated by a cover. (b) Power stability of the Tm:YLF laser when the laser system is isolated by a cover. (c) Beam quality of the Tm:YLF laser. Inset, the beam profile of the Tm:YLF laser.

Profiting from the thermal insensitive cavity design and natural negative thermo-optic coefficient of the Tm:YLF. The M^2 values of the Tm:YLF laser are measured by using a pyroelectric array cameras (Pyrocam IV) with a plano-convex lens of 400-mm focal length and a manual slide at the maximum output power of 45.85 W. The laser radiated from cavity exhibits near diffraction limit beam quality, with M^2 values of merely 1.01 and 1.05 in the horizontal and vertical directions, respectively, as shown in Fig. 4(c). Both the near field and far field spatial profiles of the laser beam are well enough, as shown in the inset of Fig. 4(c).

4. Conclusion

In conclusion, a high power continuous-wave Tm:YLF laser with high efficiency is experimentally achieved by employing double Tm:YLF crystals in a thermally insensitive resonant cavity. Under the absorbed pump power of 60.89 W, the maximum CW output power of 45.85 W is achieved, and the slope efficiency and the absorbed-to-optical conversion efficiency are 80.9% and 75.3%, respectively. In addition, the Tm:YLF laser system demonstrates an excellent performance in power stability (0.33% RMS) and beam quality (1.01×1.05). Our experiment demonstrated that the combination of employing double Tm:YLF crystals and thermally insensitive resonant cavity could improve the output power and the conversion efficiency effectively. Moreover, it is anticipated that the efficiency and output power can be enhanced further by some means, such as optimizing the resonator parameters, increasing the pump power and improving the doping concentration of Tm^{3+} ion gently. Such a high-power Tm:YLF laser is an ideal pump source for Ho:YLF and Ho:YAG crystals to obtain high-power or high-energy 2-μm laser.

Acknowledgements

Project supported by the Strategic Priority Research Program of the Chinese Academy of Sciences (Grant Nos. XDA0380205 and XDB0890101), the National Key Research and Development Program of China (Grant No. 2022YFA1604400), the National Natural Science Foundation of China (Grant Nos. 12388102, 62205351, 61925507, 62075227, 22227901, U21A20138, and 62375273), Shanghai Rising-Star Program (Grant No. 21QA1410200), the Fund from Youth Innovation Promotion Association of the Chinese Academy of Sciences (Grant No. 2020248), the Fund from Shanghai Association for Science and Technology (Grant Nos. 22DZ1100300, 22560780100, and 23560750200), China Postdoctoral Science Foundation (Grant No. GZC20232817), and Shenzhen Major Scientific and Technological Projects (Grant No. KJZD20240903100205008).

References

[1] Li Y, Chen X Y, Liu J L, Bai F, Wu C T and Jin G Y 2018 *Optik* **158** 1553
[2] Li G, Liu H J, Lu F, Wen X L, Gu Y Q and Wang Y Z 2014 *Appl. Opt.* **53** 4987
[3] Wen J, Ji Z G and Li H Z 2016 *Chin. Medi. Sci.* **31** 127
[4] Liu G, Wei D, Chen Y, Yang K, Mi S, Li J, Yang C, Wang R, Duan X, Dai T, Yao B, Ju Y and Wang Y 2020 *Infrared and Laser Engineering* **49** 12
[5] Nikitichev A A and Stepanov A I 1999 *J. Opt. Technol.* **66** 718

[6] Duan X, Yao B, Zhang Y, Song C, Ju Y and Wang Y 2008 *Chin. Opt. Lett.* **6** 591

[7] Adrian A, Venkatesan J, Sami S, M. S J, Magdalena A, Francesc D, Xavier M, Martin S and Tomas M 2023 *Appl. Phys. B* **129** 41

[8] Ding Y, Zhang D X, Wang W, Yao B Q, Duan X M, Ju Y L and Wang Y Z 2015 *Optik* **126** 855

[9] Berrou A, Collett O J P, Morris D and Esser M J D 2018 *Opt. Express* **26** 10559

[10] Demirbas U, Thesinga J, Kellert M, Kärtner F X and Pergament M 2022 *Opt. Mater. Express* **12** 4712

[11] Duan Y, Zhu H, Xu C, Ruan X, Cui G, Zhang Y, Tang D and Fan D 2016 *Opt. Express* **24** 26529

[12] Gao J, Long Q, Han Q, Wang L, Xu Z and Mao Y 2023 *Opt. Express* **31** 17175

[13] Shen J P, Lu P, Xu S C, Jiang R R, Chen Y, Chen L and Xing F Y 2024 *Chin. Phys. B* **33** 074207

[14] Mi S, Wei D, Tang J, Li J, Yao B, Yang K, Dai T and Duan X 2022 *Appl. Opt.* **61** 5755

[15] Demirbas U, Thesinga J, Beyatli E, Kellert M, Pergament M and Kärtner F X 2022 *Opt. Express* **30** 41219

[16] Tamer I, Reagan B A, Galvin T, Galbraith J, Sistrunk E, Church A, Huete G, Neurath H and Spinka T 2021 *Opt. Lett.* **46** 5096

[17] Tamer I, Reagan B A, Galvin T, Batysta F, Sistrunk E, Willard D, Church A, Neurath H, Galbraith J, Huete G and Spinka T 2022 *Opt. Express* **30** 46336

[18] Zhao J, Liu Y, Cheng P and Yu R 2023 *Chin. Opt. Lett.* **21** 031401

[19] Zhang R, Li H, Zhang P, Hang Y and Xu J 2013 *Opt. Express* **21** 20990

[20] Wang Y, Liu W, Zhang Z, Strzep A, Liu J, Chen Z, Ma F and Su L 2022 *Opt. Lett.* **47** 1117

[21] Eremeikin O N, Egorov N A, Zakharov N G, Savikin A P and Sharkov V V 2009 *J. Opt. Technol.* **76** 676

[22] Li J, Yang S H, Meissner A, Hofer M and Hoffmann D 2013 *Laser Phys. Lett.* **10** 055002

[23] Duan X M, Ding Y, Yao B Q, Dai T Y, Li Y Y and Jia F L 2014 *Chin. Phys. Lett.* **31** 074203

[24] Schellhorn M 2008 *Appl. Phys. B* **91** 71

[25] Schellhorn M, Ngcobo S and Bollig C 2009 *Appl. Phys. B* **94** 195

[26] Budni P A, Lemons M L, Mosto J R and Chicklis E P 2000 *IEEE J. Select. Top. Quantum Electron.* **6** 629

[27] Shen Y J, Yao B Q, Qian C P, Duan X M, Dai T Y and Wang Y Z 2015 *Appl. Phys. B* **118** 555

[28] Wei D S, Mi S Y, Yang K, Li J H, Tang J W, Yao B Q, Dai T Y and Duan X M 2021 *High Power Laser Science and Engineering* **9** 04000

[29] Bai F, Huang Z Z, Liu J L, Chen X Y, Wu C T and Jin G Y 2015 *Laser Phys.* **25** 075003

[30] Huang Z L, Jin G Y, Chen X Y, Wu C T and Wang L 2014 *Proceedings of SPIE – The International Society for Optical Engineering*, May 13–15, 2014, Beijing, China, p. 9298

[31] Aleshire C E, Yu C X, Reed P A and Fan T Y 2017 *Opt. Express* **25** 13408

[32] Liu X, Lu X Y, Wang H, Yan L X, Li R K, Huang W H, Tang C X, Chiche R and Zomer F 2023 *Chin. Phys. B* **32** 034206

[33] Shen J P, Chen Y, Chen L, Xing F Y, Zhang F B, Xia R Z, Zuo H Y, Xiong F and Jiang R R 2025 *Chin. Phys. Lett.* **42** 044202

[34] Na Q, Xu C, Huang Z, He M, Chen Z, Xu T, Wang L, Yan P, Li Y, Luo S and Fan D 2019 *Opt. Lett.* **44** 4403